Proceedings of the XXXII International School of Semiconducting Compounds, Jaszowiec 2003

Interlayer Coupling in EuS-Based Superlattices (Dependence on the Energy Structure of Non-Magnetic Layer)

P. Sankowski[a] and P. Kacman[b]

[a]Institute of Informatics, Warsaw University, Banacha 2, 02-097 Warsaw, Poland
[b]Institute of Physics, Polish Academy of Sciences
al. Lotników 32/46, 02-668 Warsaw, Poland

The interlayer coupling between ferromagnetic EuS layers separated by spacer layers of diamagnetic insulators, YbSe and SrS, is studied within a 3D tight-binding model. The dependencies of the coupling strength on the energy structure of the spacer, on strains resulting from the lattice mismatch between the superlattice constituents, as well as on an applied hydrostatic pressure and lattice deformations, are presented. The sign and the range of the obtained coupling agree with the behavior of magnetic correlations observed recently in neutron reflectivity spectra of EuS/YbSe superlattices.

PACS numbers: 75.70.Ak, 68.65.Cd

1. Introduction

The interlayer coupling (IC) was discovered in 1986 in Fe/Cr/Fe trilayers [1]. Since then it was observed in a variety of structures with alternating metallic ferromagnetic layers and different non-magnetic spacer layers. In the 90's this phenomenon was also discovered in all semiconductor superlattices (SLs) with antiferromagnetic, MnTe, and EuTe layers [2]. Recently, the first observation of IC between ferromagnetic, semi-insulating layers in EuS/PbS SLs has been reported [3]. The theoretical models used to explain IC in metallic structures require high density of states at the Fermi level [4] and thus are not applicable to the semiconductor structures. Among the several models tailored for all-semiconductor systems [5–9], the approach presented in [9] seems to be the most appropriate

to describe IC in the IV–VI structures and it was successfully used in [3] to explain the observed antiferromagnetic interlayer correlations in EuS/PbS SLs. This model does not assume any particular interaction mechanism, but attributes IC to the sensitivity of the SL electronic energies to the magnetic order in consecutive magnetic layers, i.e., accounts globally for the spin-dependent band structure effects.

In this paper we present the results of applying this model to the $(EuS)_m/(YbSe)_n$ and $(EuS)_m/(SrS)_n$ SLs, in which each SL period contains m magnetic and n diamagnetic molecular monolayers, perpendicular to the [001] growth direction. In these SLs the wide-gap materials ($E_g \approx 1.6$ eV for YbSe and ≈ 4.8 eV for SrS) are used as the spacer layers. In the former structure an antiferromagnetic IC was just observed [10] by neutron reflectivity measurements. This experiment, although does not allow to determine the strength of IC, has shown that the range of the coupling in these structures is shorter than that reported in [3] for EuS/PbS SLs. Efforts to grow the second considered SL are already undertaken, as EuS/SrS is a perfect candidate for studying photoinduced magnetic phenomena in ferromagnetic layers separated by an optically transparent, real insulator.

2. Theory

The magnetic material — EuS — is a classical Heisenberg ferromagnet with the Curie temperature 16.6 K. It was shown experimentally [11] that in the EuS layer structures the ferromagnetically ordered Eu spins are arranged within the layers. EuS is a semi-insulating wide-gap semiconductor. The augmented plane wave calculations of the band structure [12] show that its upper valence bands are formed mainly by anion p states, whereas the lowest conduction band is built predominantly of cation d states. The narrow $f(\uparrow)$ band is situated *ca.* 1.7 eV below the conduction band. The valence band has the maximum at the Γ point and the conduction band minimum is at the point X of the Brillouin zone. The spin splitting of the valence band results from the spin-dependent mixing of p-anion and f-cation states and the spin splitting of the conduction band is a result of f-cation and s/d-cation on-site interactions.

The II–VI compound SrS has a direct energy gap at the center of the Brillouin zone, which separates the p-anion valence bands and s-cation conduction band [13]. In [13] the band structure of SrS in the entire Brillouin zone was calculated within the self-consistent Hartree–Fock approximation. Although the calculated E_g is *ca.* 1.5 eV bigger than the value deduced from experiment, this is the best description of SrS present in the literature. Still, much less is known about the band structure of the non-magnetic YbSe — we assume that it is similar to the band structure of the magnetic EuSe, presented in [12], with neglected spin splittings (note that the only difference between ytterbium and europium atoms is that Yb

has 14, instead of the 7 for Eu, electrons in the f-shell and the orbital momentum L of these electrons vanishes in both cases).

All the components of $(EuS)_m/(YbSe)_n$ and $(EuS)_m/(SrS)_n$ SLs crystallize in the rock-salt structure, similarly to $(EuS)_m/(PbS)_n$ system. The SLs are well lattice matched — the lattice constants for EuS, YbSe, and SrS are 5.968 Å, 5.932 Å, and 6.020 Å, respectively. The strains resulting from the lattice mismatch are taken into account in the calculations — they change the strength of the IC by at most 10%. In these systems, each molecular monolayer consists of two atomic planes. For SLs grown in [111] direction these would be the cation and anion planes, but for the considered here SLs grown along the [001] crystallographic axis, each atomic plane is built of both anions and cations. In such structure every anion (cation) has 6 nearest neighbors (NN) — cations (anions) and 12 next nearest neighbors (NNN) — anions (cations).

In the tight-binding approximation the appropriate set of orbitals for every type of involved ions and the range of interactions between ions have to be chosen. The tight-binding SL parameters were obtained by adjusting the SL band structure to the energy structure of bulk EuS in the $n = 0$ limit and of bulk non-magnetic material, YbSe or SrS, in the other $m = 0$ limit. To describe Eu, Yb, and Sr ions we use s, d_{xy}, d_{xz}, d_{yz}, $d_{x^2-y^2}$, $d_{3z^2-r^2}$ orbitals, whereas to describe S and Se ions s, p_x, p_y, p_z orbitals are used. In the calculations we take into account:

- all anion–cation NN interactions,
- NNN interactions between the anions (S–S, Se–Se, S–Se),
- NNN interactions between cations (Eu–Eu, Yb–Yb, Sr–Sr, Eu–Yb, Eu–Sr).

To model the spin splittings in the valence bands of EuS we include, as second-order perturbations, the interactions of anion $p(\uparrow)$ orbitals with $f(\uparrow)$ cation orbitals. The interaction with $f(\downarrow)$ orbitals are neglected due to much bigger energetic distance. To reproduce the spin splittings in the conduction bands we use two on-site exchange constants: J_s for s orbitals and J_d for d orbitals. The tight-binding parameters of EuS are determined by a fit to the structure reported in [12]. To get the tight-binding parameters for SrS we fitted the model band structure to the results presented in [13]. The YbSe bands are simulated by the known structure of EuSe [12] with neglected spin splittings and the cation parameters re-scaled according to the Harrison rules [14].

3. Results

The obtained band structures are presented in Fig. 1. From Fig. 1 one can see that in contrast to the situation in EuS/PbS SLs, where the EuS magnetic layers formed high (≈ 1 eV) potential barriers for electrons, in the studied here SLs one can expect that barriers in the conduction band are formed by the spacer layers — in the case of YbSe small, but for SrS as high as $\approx 2{-}3$ eV. The interactions at the

interfaces and the real band-offsets can change the final scheme of the electronic bands of EuS/YbSe SL, but one can hardly imagine that they will reduce the non-magnetic barriers in EuS/SrS SLs. To estimate the parameters describing interactions at the interfaces, i.e., between non-magnetic and magnetic cations, and between the different, S and Se, anions, we used the Harrison interatomic matrix elements. Moreover, the Harrison relations for the NNN parameters ($pp\sigma = -4pp\pi$ and $dd\sigma = -2dd\pi$) were used to reduce the number of independent parameters. In all calculations we neglected the spin–orbit terms.

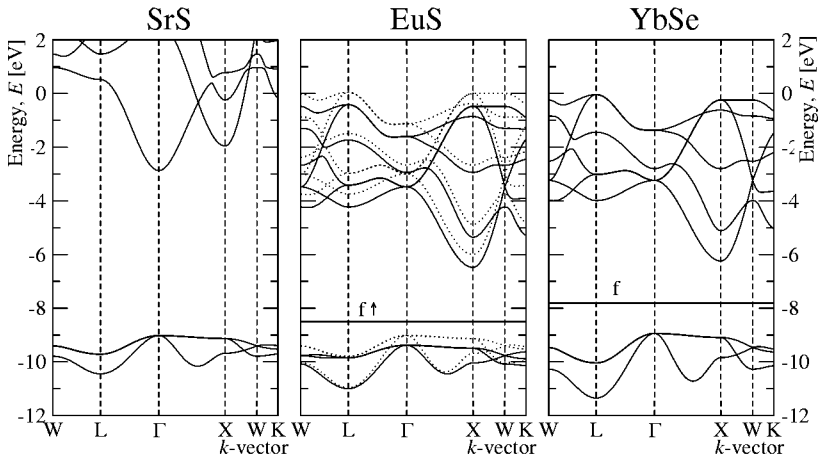

Fig. 1. Tight-binding model band structures of SrS, EuS, and YbSe. For EuS, the solid lines represent the "spin up" bands and the dotted — "spin down" bands. The position of the f-band in YbSe cannot be inferred from the EuSe structure — it is just drawn at the distance 1.6 eV (experimentally estimated E_g) below the conduction band.

In order to calculate the interlayer coupling the total energies of the valence electrons for two different SLs, one with the same (ferromagnetic) and the other with opposite (antiferromagnetic) spin configurations in consecutive magnetic layers, were compared (see Fig. 2). The difference between these two energies per unit surface of the layer, ΔE, was considered as a measure of the strength of the interlayer magnetic coupling resulting from band structure effects. Thus, to construct the Hamiltonian matrix one has to consider the SL magnetic cell containing two magnetic layers. This elementary magnetic cell consists of $2(n + m)$ monolayers, i.e., of $2(m + n)$ anions, $2m$ magnetic cations and $2n$ non-magnetic cations.

In both studied types of SLs the calculations show that the antiferromagnetic alignment of magnetization vectors in successive magnetic layers is energetically preferred — in agreement with the experimental findings in EuS/YbSe SLs obtained in [10]. We have performed the calculations for a number of SL with varying m and n. The calculations show that in these SLs, as in EuS/PbS systems, the IC depends marginally on the magnetic layer thickness m, i.e., that the coupling is

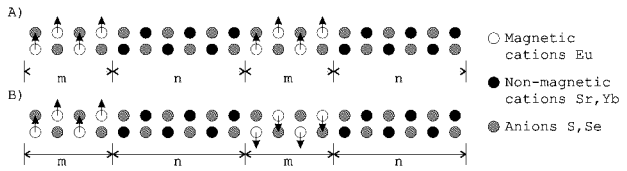

Fig. 2. SL with the spins in successive ferromagnetic layers aligned (A) ferromagnetically and (B) antiferromagnetically.

primary an interface effect even when the band structures of the SL constituent materials are very similar, like for EuS/YbSe SLs. In Fig. 3 the dependence of the IC on the non-magnetic layer thickness n is presented and compared with the IC in EuS/PbS structures (the IC strength is described by the constant $J_1 = \Delta E/4$, commonly used for the ferromagnetic metallic multilayers [15]). The strength of the coupling in all three cases decreases exponentially with n, but with different speed, i.e., the obtained range of the coupling depends on the spacer material. For EuS layers separated by YbSe the calculated range of the IC is smaller than in EuS/PbS SLs, again in agreement with the experimental result.

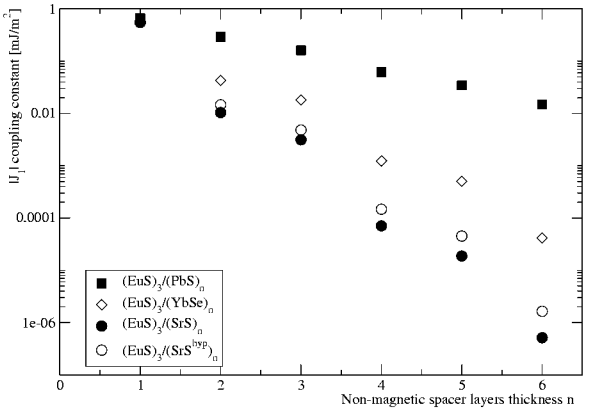

Fig. 3. The interlayer coupling constant J_1 as a function of spacer thickness for $(\mathrm{EuS})_m/(\mathrm{YbSe})_n$, $(\mathrm{EuS})_m/(\mathrm{SrS})_n$ and $(\mathrm{EuS})_m/(\mathrm{PbS})_n$ SLs. The small deviations of J_1 for every second n result from layer stacking. For the $(\mathrm{EuS})_m/(\mathrm{SrS}^{\mathrm{hyp}})_n$ see discussion after Fig. 4.

To study the origin of the change of the IC range for different spacers, we made a series of calculations for hypothetical diamagnetic materials, which have the same structure as PbS and SrS, but different energy gaps. The change of the energy gap is obtained by moving the on-site energies for the conduction band orbitals. By this study we wanted also to check how the much too large value for E_{g} in SrS, taken after [13], changes the result for EuS/SrS SL. The results presented in Fig. 4 show that the IC constant depends strongly on the diamagnetic

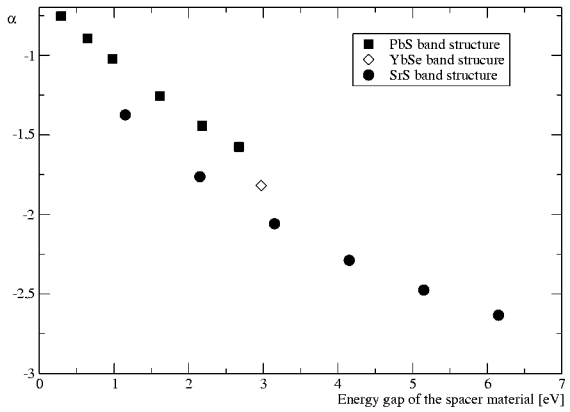

Fig. 4. The rate α of the decrease in the interlayer coupling constant J_1 with the spacer thickness ($J_1 = A\exp(\alpha n)$) as function of the energy gap of the hypothetic non-magnetic spacers.

spacer's energy gap, but changes also for materials with different band structures — the coupling depends on the spin-dependent mixing of the states, which in turn depends on the energy distances between bands consisting of, e.g., p and d orbitals. For the SrS structure, the reduction of E_g to the experimentally established value 4.8 eV would lead to an increase in the calculated IC — the results for such EuS/SrS^{hyp} SLs are shown in Fig. 3 by open circles.

Finally, we have also investigated the dependence of IC on strain and on applied hydrostatic pressure, which are known to influence importantly the magnetic properties of magnetic multilayer structures [16]. A question arises whether can the strain, neglected in [9], be responsible for the fact that the experimentally deter-

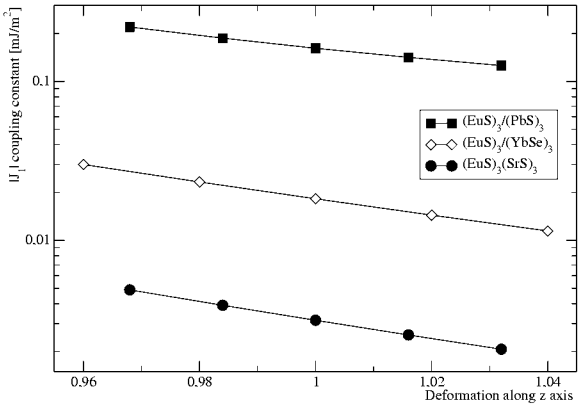

Fig. 5. The dependence of interlayer coupling constant J_1 on the deformation of the SL along the z-axis.

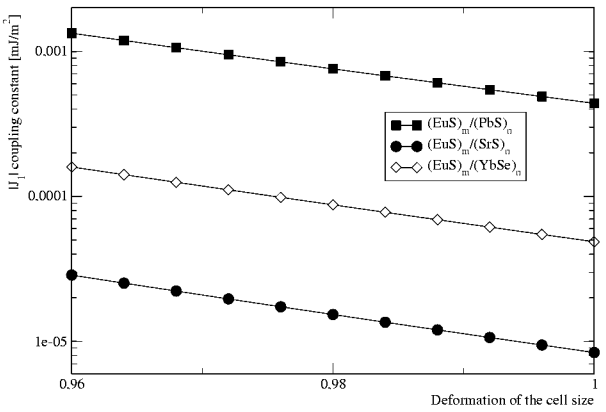

Fig. 6. The interlayer coupling constant J_1 versus the size of the SL elementary cell.

mined IC in EuS/PbS is about an order of magnitude smaller than the calculated values [3]. A very simple model, in which the strain was applied by deforming the SL lattice along the growth z-axis and the hydrostatic pressure was simulated by a change of the size of the SL cell, was used. In agreement with the intuition, the strength of the IC increases for deformations, which decrease the distance between magnetic layers, as shown in Figs. 5 and 6. Although the possible deformations can change the IC by factor of two, as one can see in the figures, this is not enough to explain the above mentioned discrepancy, which has to be probably also ascribed to the interface roughness and interdiffusion.

4. Conclusion

In conclusion, we have shown that the spin-dependent energy structure effects can lead to the coupling between semiconductor ferromagnetic EuS layers not only when the spacer layers form wells in the energy structure of the multilayer (like in EuS/PbS SLs) but also when they are insulating materials and their band structure is either similar to EuS (EuS/YbSe) or they introduce high potential barriers for the electrons (EuS/SrS). The calculated coupling is antiferromagnetic and the shorter in range the larger is the energy gap of the diamagnetic spacer, in qualitative agreement with the recent experimental findings.

Acknowledgments

This work is supported by projects: FENIKS project (EC:G5RD-CT-2001-00535), Ohno Semiconductor Spintronics ERATO Project of Japan Science and Technology Corporation, and the State Committee for Scientific Research grant PBZ-KBN-044/P03/2001.

References

[1] P. Grünberg, R. Schreiber, Y. Pang, M.B. Brodsky, H. Sowers, *Phys. Rev. Lett.* **57,** 2442 (1986).

[2] T.M. Giebultowicz, V. Nunez, G. Springholz, G. Bauer, J. Chen, M.S. Dresselhaus, J.K. Furdyna, *J. Magn. Magn. Mater.* **140-144,** 635 (1995); V. Nunez, T.M. Giebultowicz, W. Faschinger, G. Bauer, H. Sitter, J.K. Furdyna, *ibid.*, p. 633; J.J. Rhyne, J. Lin, J.K. Furdyna, T.M. Giebultowicz, *J. Magn. Magn. Mater.* **177-181,** 1195 (1998).

[3] H. Kępa, J. Kutner-Pielaszek, J. Blinowski, A. Twardowski, C.F. Majkrzak, T. Story, P. Kacman, R.R. Galazka, K. Ha, H.J.M. Swagten, W.J.M. de Jonge, A.Yu. Sipatov, V. Volobuev, T.M. Giebultowicz, *Europhys. Lett.* **56,** 54 (2001).

[4] P. Bruno, *Phys. Rev. B* **52,** 411 (1995); cond-mat/9905022.

[5] P. Shevchenko, L. Świerkowski, J. Oitmaa, *J. Magn. Magn. Mater.* **177-181,** 1168 (1998).

[6] T.M. Rusin, *Phys. Rev. B* **58,** 2107 (1998).

[7] M. Wilczyński, R. Świrkowicz, *Phys. Status Solidi B* **212,** 165 (1999).

[8] V.K. Dugaev, V.I. Litvinov, W. Dobrowolski, T. Story, *Solid State Commun.* **110,** 351 (1999).

[9] J. Blinowski, P. Kacman, *Phys. Rev. B* **64,** 045302 (2001).

[10] H. Kępa, P. Sankowski, P. Kacman, A.Yu. Sipatov, C.F. Majkrzak, T.M. Giebultowicz, to be presented at ICM2003, Rome (2003).

[11] A. Stachow-Wojcik, T. Story, W. Dobrowolski, M. Arciszewska, R.R. Galazka, M.W. Kreijveld, C.H.W. Swüste, H.J.M. Swagten, W.J.M. de Jonge, A. Twardowski, A.Yu. Sipatov, *Phys. Rev. B* **60,** 15220 (1999).

[12] S.J. Cho, *Phys. Rev. B* **1,** 4589 (1970).

[13] R. Pandey, J.E. Jaffe, A. Barry Kunz, *Phys. Rev. B* **43,** 9228 (1991).

[14] W.A. Harrison, *Electronic Structure and the Properties of Solids*, W.H. Freeman and Co., San Francisco 1980.

[15] S.S.P. Parkin, *Phys. Rev. Lett.* **67,** 3598 (1991).

[16] T. Story, *Phys. Status Solidi B* **236,** 310 (2003) and the references therein.